Hindawi
Journal of Robotics
Volume 2023, Article ID 9768653, 1 page
https://doi.org/10.1155/2023/9768653

Retraction

Retracted: Recognition and Modeling of Crisis Propagation Patterns Combined with Robot Simulation of Social Networks

Journal of Robotics

Received 8 August 2023; Accepted 8 August 2023; Published 9 August 2023

This article has been retracted by Hindawi following an investigation undertaken by the publisher [1]. This investigation has uncovered evidence of one or more of the following indicators of systematic manipulation of the publication process:

(1) Discrepancies in scope
(2) Discrepancies in the description of the research reported
(3) Discrepancies between the availability of data and the research described
(4) Inappropriate citations
(5) Incoherent, meaningless and/or irrelevant content included in the article
(6) Peer-review manipulation

The presence of these indicators undermines our confidence in the integrity of the article's content and we cannot, therefore, vouch for its reliability. Please note that this notice is intended solely to alert readers that the content of this article is unreliable. We have not investigated whether authors were aware of or involved in the systematic manipulation of the publication process.

Wiley and Hindawi regrets that the usual quality checks did not identify these issues before publication and have since put additional measures in place to safeguard research integrity.

We wish to credit our own Research Integrity and Research Publishing teams and anonymous and named external researchers and research integrity experts for contributing to this investigation.

The corresponding author, as the representative of all authors, has been given the opportunity to register their agreement or disagreement to this retraction. We have kept a record of any response received.

References

[1] Y. Wang, "Recognition and Modeling of Crisis Propagation Patterns Combined with Robot Simulation of Social Networks," *Journal of Robotics*, vol. 2022, Article ID 3454396, 12 pages, 2022.

Hindawi
Journal of Robotics
Volume 2022, Article ID 3454396, 12 pages
https://doi.org/10.1155/2022/3454396

Research Article

Recognition and Modeling of Crisis Propagation Patterns Combined with Robot Simulation of Social Networks

Yafei Wang

Department of Basic Education, Huanghe Jiaotong University, Jiaozuo 454000, China

Correspondence should be addressed to Yafei Wang; 2016090302@zjtu.edu.cn

Received 13 August 2022; Revised 1 September 2022; Accepted 24 September 2022; Published 11 October 2022

Academic Editor: Shahid Hussain

In order to improve the identification effect of a crisis propagation mode, this paper studies the crisis propagation mode of social networks and uses an intelligent method to identify the crisis propagation mode. Moreover, this paper analyzes and deduces the features of the modulated signal from the two aspects of spectrum and autocorrelation functions and extracts and simulates the features of signals of different modulation types. In addition, this paper verifies the proposed recognition method from two aspects through theoretical experiments and measured data and builds an intelligent model. Through the experimental research, it can be seen that the identification effect and the control effect of the crisis propagation model based on the social network proposed in this paper are relatively obvious.

1. Introduction

In the real world, the phenomenon of coevolving crisis communication between different crisis communication processes is common. It is also a huge challenge for scholars to model and analyze these complicated coevolving crisis communication processes and propose corresponding and feasible intervention strategies.

The security and privacy-hidden dangers in social networks have brought trouble to users, which has attracted the attention of researchers [1]. For example, on a social platform, when it comes to sensitive topics such as money transactions and privacy disclosure, users need to clearly judge the trustworthiness of the other user. For another example, when a mobile social network is applied to a location-based service, people pay particular attention to how private information such as location is known to surrounding users. That is, when a user displays or hides location information from other individual users or a specific group, an appropriate security level needs to be set [2]. Interactions in social networks sometimes occur between unfamiliar users, and on social platforms, sensitive interactions such as economics or privacy often occur, so trust plays an important role. It can be said that the normal operation of a social network depends on the level of trust among users, and the trust among users in a real social network is the basis of people's communication [3].

It is particularly important to study an appropriate trust relationship model to ensure the security of social networks. Specifically, users need to measure the degree of trust in other users to decide how to disclose and share personal privacy information and how to choose which users to interact with. However, the existing social network trust models still have certain drawbacks; for example, there is no clear description of the calculation rules of trustworthiness (quantitative representation of trust). A trust model based on semiring algebra theory is proposed [4], which can well describe credibility calculation rules and can express other trust models flexibly, so it becomes a very important trust model. Literature [5] proposed a trust path search algorithm and established a semiring trust model for privacy protection. However, the trust model still has some shortcomings, such as it does not define and describe the time-based dynamic change problem. One of the typical characteristics of the social network is its dynamic nature, for example, users are added and deleted at any time in social networks. In this way, the topology of the network changes at any time, causing changes in the links between nodes, and the user's

trust is propagated and calculated through the links between users so that the user's trust will also have dynamic variability [6]. Therefore, from an objective point of view, the trust model for calculating user credibility needs to reflect this dynamic nature, timely reflect changes in users' behavior, and improve adaptability.

Identifying key users in a network is an important research content for complex networks, including social networks. For example, in various social networks, it is often necessary to know which users are the most active and influential, in order to provide a useful basis for the content distribution of mobile social networks or to provide operators with guidance on marketing strategies [7]. In social network analysis, "centrality" is used to describe the importance of nodes in the network [8]. Establishing an accurate centrality measurement model is an important method to identify key users. Early network research did not consider the weight of links between users, but only whether users were connected. This will lose a lot of network information, resulting in inaccurate centrality measures. In recent years, researchers have found that in order to more accurately identify key users, it is necessary to integrate the weights into the links between users (such as link strength, intimacy, and credibility), and such a social network is called a weighted social network [9].

An important feature of social networks is that they consist of multiple communities. Then, the most important nodes in a social network should belong to different communities. The centrality measurement method of the above weighted network has certain defects because it cannot effectively identify the important nodes of each community in the social network [10]. Since weighted networks can be viewed as multigraphs mapped into unweighted networks, the classical centrality measures of weighted networks inherit their weaknesses in unweighted networks. Degree centrality is the simplest method that only considers localized structural information but does not consider the global structure of the network, including multicommunity features [11]. Then, the dominant nodes ranked based on degree centrality are likely not the most influential nodes in each community. The closeness and betweenness centrality of weighted networks is based on the shortest path algorithm with the limitation that nodes that are not on the shortest path between any two other nodes will have the same centrality value (i. e. 0) [12]. Then, when applied to large sparse networks, the effective centrality values for most nodes will not be available based on them. More importantly, they do not explicitly state the relationship between centrality and community structure. Based on EVC, the most influential nodes are clustered in a community in a weightless network, which also suffers from the same flaws in a weighted network [13].

The dissemination of information on the real network can affect all aspects of human society. In view of the fact that most of the current theoretical analysis methods of information dissemination on complex networks are based on nodes and the theoretical research based on network edges is still relatively lacking, a set of information dissemination analysis methods based on the dynamic state of edges has been developed [14]. Based on this, an indicator is proposed to measure the influence of potential connections in promoting information dissemination. This indicator can effectively screen out the optimal potential links that can promote information dissemination in the network. In addition, based on the analysis of the optimal latent edge, literature [15] proposed an information propagation intervention strategy based on the optimal latent edge. A set of theoretical analysis methods of information propagation based on the dynamic state of the connection edge is developed, and a propagation intervention strategy that combines the characteristics of the network structure in the network propagation dynamic system and the characteristics of propagation dynamics itself is proposed.

Compared with single information propagation, information-information coevolution propagation has a more complex evolution mechanism, and its corresponding theoretical research is still rare. It is very challenging to effectively intervene in information-information coevolution propagation dynamics on complex networks by combining the characteristics of network structure and propagation dynamics themselves [16]. Literature [17] proposed an index to quantitatively describe the influence of potential connections of the network in promoting information-information coevolution propagation, aiming at the symmetrical propagation of two types of information in the coevolution system. Literature [18] proposed an information-information coevolution propagation intervention strategy based on optimal latent connections. The strategy effectively combines the structural characteristics of the network in the coevolution propagation system and the characteristics of coevolution propagation dynamics itself and is better than the heuristic strategy that only relies on the network topology centrality in intervening information-information coevolution propagation on the network. In this paper, the information-information co-evolution propagation mechanism on complex networks is studied, and a coevolution propagation intervention strategy that effectively combines the characteristics of the network structure and propagation dynamics is proposed for the symmetrical propagation of two types of information in the coevolution system.

This paper studies the crisis communication mode of the social network, identifies the crisis communication mode through intelligent methods, and builds an intelligent model to promote the effective control of crisis communication.

2. Artificial Feature Parameter Extraction for Social Network Crisis Data Recognition

2.1. Signal Extraction. The theory of signal feature extraction from social network crisis data has been greatly complemented by decades of research. The earliest used feature parameters are the features obtained based on the instantaneous information of the signal. This feature is greatly disturbed by noise and has almost no classification effect on the signal under the condition of a low signal-to-noise ratio. The feature parameters used in this paper are divided into three categories, with a total of 11 kinds, and all feature vectors are shown in Figure 1.

The time-domain waveform of a social network crisis data signal contains a lot of instantaneous information about the signal. By analyzing and calculating the waveform of the social network crisis data signal, the signal amplitude, frequency, phase, and other information can be obtained, which constitute the most basic features of the social network crisis data signal.

The signal used in the experiment is a complex signal, and the signal is modeled as an analytical signal $s(t)$ before the experiment:

$$s(t) = x(t) + jy(t). \tag{1}$$

The imaginary part in the analytical expression $s(t)$ is the Hilbert transform of the real signal $x(t)$. The Hilbert transform is different from the Fourier transform. The signal after the Fourier transform maintains positive and negative frequencies and carries redundant information. The Hilbert transform can eliminate redundant frequencies and reduce frequency band occupation. The analytical expression $s(t)$ of the signal is sampled at the sampling frequency f_s, and the sampled signal is expressed as follows:

$$s(i) = x(i) + jy(i) = A(i)e^{\phi(i)}. \tag{2}$$

Among them, $A(i)$ represents the instantaneous amplitude sequence of the signal, which is expressed as follows:

$$A(i) = \sqrt{\left(x^2(i) + y^2(i)\right)}. \tag{3}$$

The instantaneous phase in the experiment is denoted by the unfolded phase, and $\phi(i)$ represents the unfolded phase sequence of the signal. $\theta(i)$ is the instantaneous phase sequence, and according to the inverse trigonometric function, $\theta(i)$ can be expressed as follows:

$$\theta(i) = \begin{cases} \arctan\left[\dfrac{y(i)}{x(i)}\right], x(i) > 0, \\ \arctan\left[\dfrac{y(i)}{x(i)}\right] - \pi, x(i) < 0, y(i) \le 0, \\ \arctan\left[\dfrac{y(i)}{x(i)}\right] + \pi, x(i) < 0, y(i) > 0, \\ -\dfrac{\pi}{2}, x(i) = 0, y(i) \le 0, \\ \dfrac{\pi}{2}, x(i) = 0, y(i) > 0. \end{cases} \tag{4}$$

The value range of the folding phase $\theta(i)$ is between $(-\pi, \pi)$. The phase used in the experiment is the unfolded phase, and the unfolded phase $\phi(i)$ needs to be obtained from $\theta(i)$ through phase correction. The correction sequence $C(i), C(i)$ used in this process is as follows:

$$C(i) = \begin{cases} C(i-1) - 2\pi, \theta(i+1) - \theta(i) > \pi, \\ C(i-1) + 2\pi, \theta(i) - \theta(i+1) > \pi, \\ C(i-1), \text{others}. \end{cases} \tag{5}$$

According to the above definition, the first value $C(1)$ in the correction sequence cannot be given and the default $C(1)$ is 0. The unfolded instantaneous phase $\phi(i)$ is obtained by adding the folded phase sequence and the modified sequence:

$$\phi(i) = \theta(i) + C(i). \tag{6}$$

The frequency of the continuous signal is differential of the phase. In the sampled signal, the differential relationship is used instead of the differential relationship. The instantaneous frequency $f(i)$ can be defined as follows:

$$f(i) = \frac{1}{2\pi T_s}[\phi(i) - \phi(i-1)]. \tag{7}$$

Among them, T_s is the sampling period.

After obtaining the instantaneous amplitude, instantaneous phase, and instantaneous frequency of the social network crisis data signal, four instantaneous features based on the above three basic information are calculated according to statistical principles. They are the maximum spectral density $\gamma_{\max}$ of the amplitude based on the envelope amplitude, the standard deviation δ_{aa} of the absolute value of the amplitude that is more distinguishable in the high-order social network crisis data type, the standard deviation δ_{ap} of the absolute value of the amplitude, which is more distinguishable in the high-order social network crisis data type, the standard deviation of the absolute value of the phase based on the phase information, and the standard deviation δ_{af} of the absolute value of the frequency based on the frequency information.

The social network crisis data signals based on the amplitude social network crisis data are quite different in the instantaneous amplitude of the envelope, and the amplitude modulation signals of different social network crisis data parameters can be distinguished by using statistical features based on the instantaneous amplitude. This paper mainly uses two statistical features based on the instantaneous amplitude, which are the normalized amplitude maximum spectral density $\gamma_{\max}$ and the normalized amplitude absolute value standard deviation δ_{aa}.

2.1.1. Normalized Amplitude Maximum Spectral Density γ_{max}. $\gamma_{\max}$ is a feature that can distinguish the envelope fluctuation information. $\gamma_{\max}$ can sense small changes in the signal envelope, and the obvious envelope changes are the MASK signal and the MQAM signal. At the same time, the MFSK signal and the MPSK signal also produce subtle envelope changes when the phase is discontinuous. According to formula (3), the instantaneous amplitude sequence $A(i)$ of the social network crisis data signal is obtained, and the instantaneous amplitude average value m_a is calculated as follows:

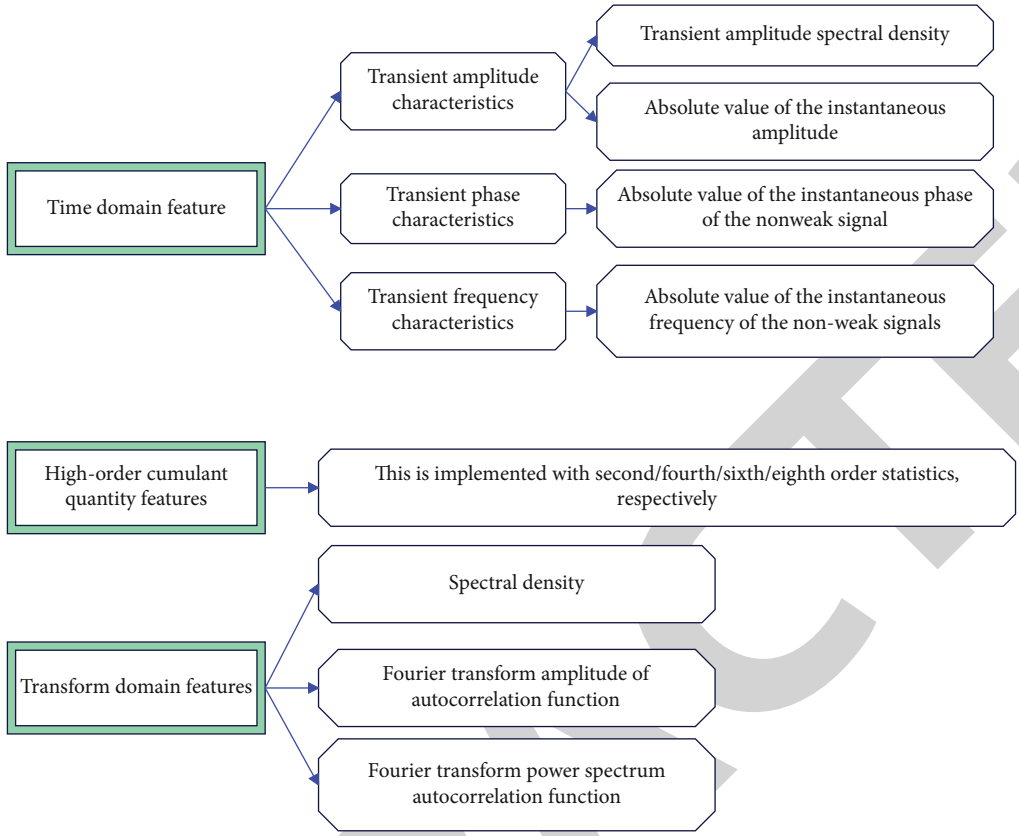

Figure 1: Feature parameters of social network crisis data recognition.

$$m_a = \frac{1}{N_s}\sum_{i=1}^{N} A(i). \tag{8}$$

Among them, N_s represents the number of sampling points, and the zero-center normalization of $A(i)$ is performed to obtain $A_{cn}(i)$:

$$A_n(i) = \frac{A(i)}{m_a}, \qquad A_{cn}(i) = A_n(i) - 1. \tag{9}$$

The normalized amplitude maximum spectral density $\gamma_{\max}$ of the signal is defined by $A_{cn}(i)$, which is as follows:

$$\gamma_{\max} = \frac{\max\left|\mathrm{FFT}\left[A_{cn}(i)\right]\right|^2}{N_s}. \tag{10}$$

Figure 2 shows the normalized magnitude maximum spectral density feature $\gamma_{\max}$ of 13 signal social network crisis data types as a function of the signal-to-noise ratio SNR. The $\gamma_{\max}$ feature is generated based on the instantaneous amplitude and has a good effect on distinguishing the MASK signals that have changes in amplitude during the social network crisis data process and can completely separate the 2ASK, 4ASK, and 8ASK signals from the rest of the signals. When the SNR > 10 dB, the feature $\gamma_{\max}$ can distinguish the 2PSK signal and the 8QAM signal at the same time, and the feature $\gamma_{\max}$ of the remaining signals is similar but different.

2.1.2. Normalized Amplitude Absolute Value Standard Deviation δ_{aa}. δ_{aa} is the feature used to describe the absolute amplitude information of the social network crisis data signal. By calculating the amplitude absolute value deviation of different amplitude modulation signals, δ_{aa} completes the classification of the signals with obvious changes in the absolute value of the envelope. δ_{aa} is particularly effective in identifying high-order signals, which can distinguish different signals such as MASK and MQAM.

$$\delta_{aa} = \sqrt{\frac{1}{N_s}\left(\sum_{i=1}^{N_s} A_{cn}^2(i)\right) - \left(\frac{1}{N_s}\sum_{i=1}^{N_s}\left|A_{cn(i)}\right|\right)^2}. \tag{11}$$

Figure 3 describes the distribution of the feature δ_{aa} of 13 social network crisis data signals under different signal-to-noise ratios, and δ_{aa} is used to characterize the absolute instantaneous amplitude information of the signal, which is clearly distinguished from high-order amplitude-modulated signals. When SNR > 6 dB, the feature δ_{aa} can successfully distinguish MASK signals. At the same time, the feature δ_{aa} is able to distinguish the MQAM signal under a high signal-to-noise ratio.

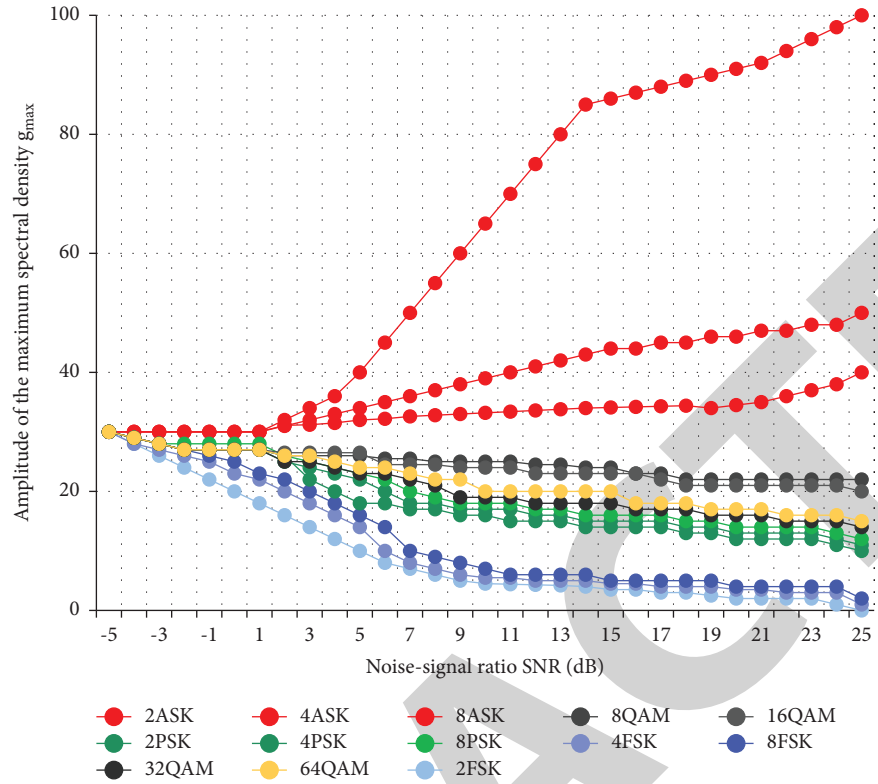

Figure 2: A variation curve of the feature γ_{max} with the signal-to-noise ratio under different social network crisis data methods.

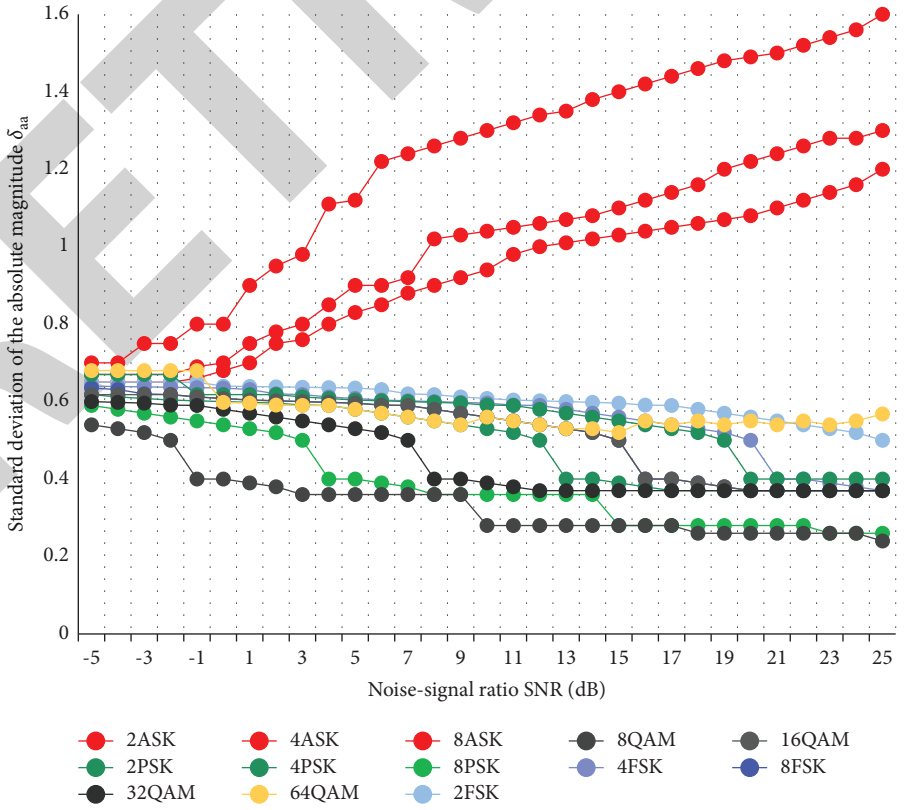

Figure 3: A variation curve of the feature δ_{aa} with the signal-to-noise ratio under different social network crisis data methods.

The standard deviation δ_{ap} of the phase absolute value is a feature that characterizes the instantaneous phase absolute value of the social network crisis data signal. It is used to distinguish signals with large changes in absolute phase information and has a better effect on high-order MPSK signals. First, we perform zero centering on the phase information.

$$\phi_{NL}(i) = \phi(i) - \frac{2\pi f_c i}{f_s}. \tag{12}$$

In order to ensure the accuracy of the calculation results, the signal segment with strong energy is selected for detection, and the strong and weak signal judgment threshold a_t is set; the feature δ_{ap} is expressed as follows:

$$\delta_{ap} = \sqrt{\frac{1}{C}\left(\sum_{A_n(i) > a_t} \phi_{NL}^2(i)\right) - \left(\frac{1}{C}\sum_{A_n(i) > a_t} \left|\phi_{NL}(i)\right|\right)^2}. \tag{13}$$

f_c and f_s represent the carrier frequency and sampling frequency of the signal, respectively, and C represents the number of signal values that satisfy the nonweak signal decision threshold.

Figure 4 describes the distinction between different signals by δ_{ap}. In the case of SNR > 15 dB, the feature δ_{ap} can accurately distinguish the 2PSK signal and the 4PSK signal, but the 8PSK signal and the rest of the signals produce feature aliasing. Affected by noise, feature δ_{ap} is not highly discriminative to MPSK signals at the low SNR.

The standard deviation δ_{af} of the absolute value of frequency is used to represent the frequency information of social network crisis data signals, which is used to distinguish the social network crisis data signals that are different in the frequency dimension. First, the frequency information is processed to obtain the zero-center normalized frequency $f_N(i)$:

$$m_f = \frac{1}{N_s}\sum_{i=1}^{N_s} f(i) f_n(i) = f(i) - m_f f_N(i) = \frac{f_n(i)}{r_b}. \tag{14}$$

Among them, r_b is the signal rate, and δ_{af} is defined as follows:

$$\delta_{af} = \sqrt{\frac{1}{C}\left(\sum_{A_n > a_t} f_N^2(i)\right) - \left(\frac{1}{C}\sum_{A_n > a_t} \left|f_N(i)\right|\right)^2}. \tag{15}$$

Figure 5 shows the variation of the feature δ_{af} with the signal-to-noise ratio of different social network crisis data methods. It can be seen from the figure that the feature δ_{af} of the MFSK signal is obviously different from other social network crisis data methods, and the feature δ_{af} has a good distinguishing effect on the 2ASK signal when the SNR > 5 dB.

2.2. Higher Order Cumulant Feature Parameters. Another feature used in the study is based on HOC generation, the cumulant of Gaussian white noise is zero, and the high-order cumulant feature can reduce the interference of Gaussian white noise on the signal. Higher order cumulants are an important part of higher order statistical theory. Higher order statistical theory is aimed at statistics above the second order, and its main contents include higher order moments, higher order cumulants, and higher order spectra. The purpose of signal identification is achieved by calculating the cumulative amounts of different social network crisis data signals at various stages and using different settings of the cumulative amounts to distinguish the thresholds of social network crisis data signals. At present, the recognition algorithms based on HOC usually use second-order, fourth-order, and sixth-order cumulants, and cumulants higher than tenth-order are not often used due to the complexity of calculation. In the experiment, the features based on HOC are obtained by the composite use of the second-order, fourth-order, sixth-order, and eighth-order cumulants.

For a continuous random variable x, its probability density function is $f(x)$. The mathematical expectation of the function $g(x)$ is as follows:

$$E\{g(x)\}^{\text{def}} = \int_{-\infty}^{\infty} f(x) g(x) \mathrm{d}x. \tag{16}$$

In particular, when $g(x) = e^{j\omega x}$, there is

$$\phi(\omega)^{\text{def}} = E\left\{e^{i\omega x}\right\} = \int_{-\infty}^{\infty} f(x) e^{j\omega x} \mathrm{d}x. \tag{17}$$

$\phi(\omega)$ is called the first characteristic function. The k-order origin moment m_k and central moment μ_k of a random continuous variable x are defined as follows:

$$\begin{aligned} m_k^{\text{def}} &= E\left\{x^k\right\} = \int_{-\infty}^{\infty} x^k f(x) \mathrm{d}x, \\ \mu_k^{\text{def}} &= E\left\{(x-\eta)^k\right\} = \int_{-\infty}^{\infty} (x-\eta)^k f(x) \mathrm{d}x. \end{aligned} \tag{18}$$

Among them, $\eta = E\{x\}$ represents the first moment of the random variable x. Since the random variable x has zero mean, its k-order origin moment and central moment are equivalent. We set $\omega = 0$ and use the k-th derivative of the first eigenfunction to obtain the k-th moment of x:

$$m_k = E\left\{x^k\right\} = (-j)^k \frac{d^k \phi(\omega)}{d\omega^k}\Big|_{\omega=0} = (-j)^k \phi^{(k)}(0). \tag{19}$$

The k-th order moment of the random variable x is generated by the first characteristic function, and $\phi(\omega)$ is also called the moment generating function. The natural logarithm $\psi(\omega)$ of $\phi(\omega)$ is called the second characteristic function, denoted as follows:

$$\psi(\omega)^{\text{def}} = \ln \phi(\omega). \tag{20}$$

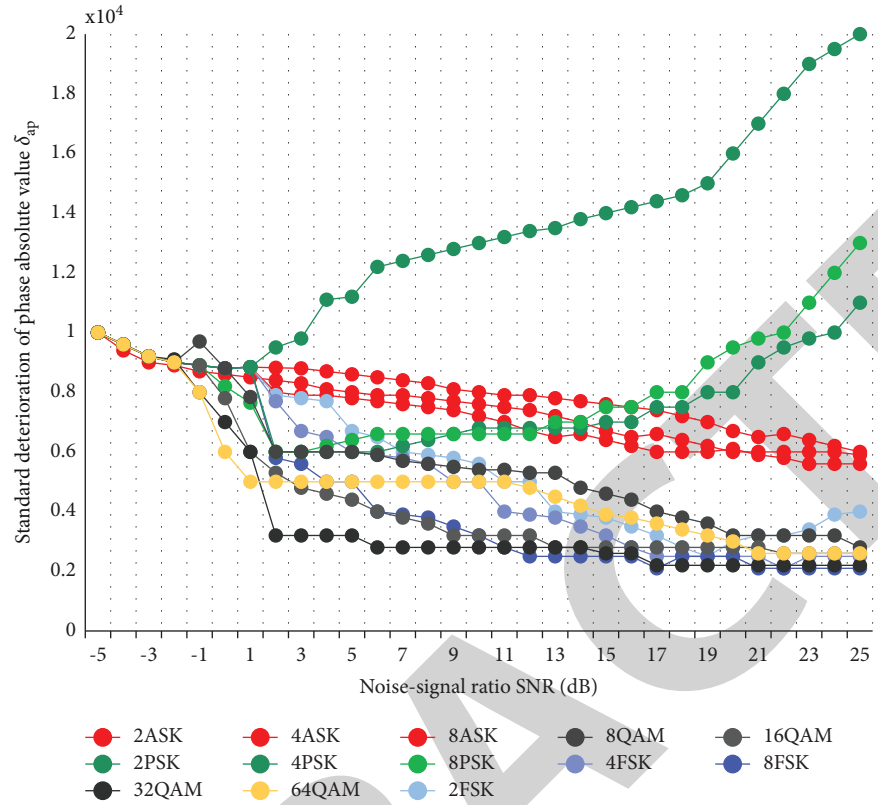

Figure 4: A variation curve of the feature δ_{ap} with the signal-to-noise ratio under different social network crisis data methods.

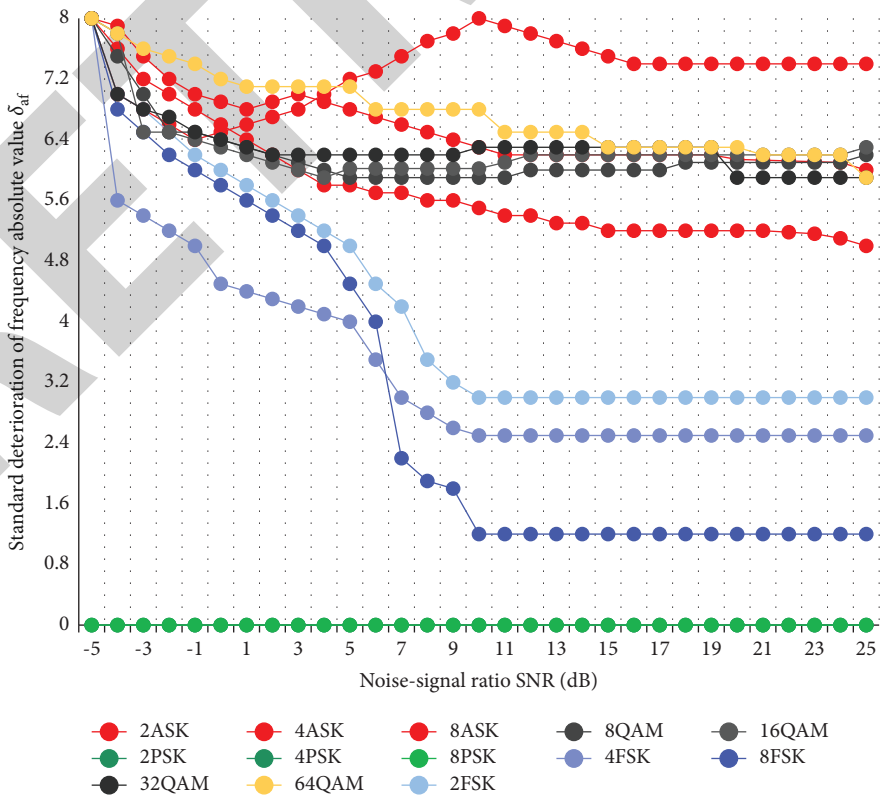

Figure 5: A variation curve of the feature δ_{af} with the signal-to-noise ratio under different social network crisis data methods.

Similar to the definition of the k-order moment, the k-order cumulant of the random variable x can be defined as follows:

$$c_{kx} = (-j)^k \frac{d^k \ln \phi(\omega)}{d\omega^k}|_{\omega=0} = (-j)^k \psi^{(k)}(0). \tag{21}$$

The second characteristic function is also called the cumulant generating function.

The moment and cumulant are used to calculate the high-order cumulant feature. For the stationary continuous random signal $X(t)$, we set $X_1 = X(t), X_2 = X(t+\tau_1), \ldots\ldots, X_k = X(t+\tau_{k-1})$ and define the k-order cumulant of the random signal as follows:

$$C_{kx}(\tau_1, \tau_2, \ldots\ldots \tau_{k-1}) = \mathrm{Cum}\{X(t), X(t+\tau_1), \ldots\ldots, X(t+\tau_{k-1})\}. \tag{22}$$

Its k-order mixing moment can be expressed as follows:

$$M_{km} = E\left[X(t)^{k-m} X^*(t)^m\right]. \tag{23}$$

Among them, $X^*(t)$ represents the conjugation of $X(t)$. Higher order moments and cumulants have the following conversion relationship:

$$\mathrm{Cum}[X_1, X_2, \ldots\ldots, X_k] = \sum (-1)^{q-1}(q-1)! \prod_{p=1}^{q} E\left\{\prod_{i\in U_p} X_i\right\}. \tag{24}$$

The higher order cumulant of a zero-mean stationary complex random process $X(t)$ is expressed as follows:

The second-order cumulant is

$$\begin{aligned} C_{20} &= \mathrm{Cum}(X, X) = M_{20} = E[X(t)X(t)], \\ C_{21} &= \mathrm{Cum}(X, X^*) = M_{21} = E[X(t)X^*(t)]. \end{aligned} \tag{25}$$

The fourth-order cumulant is

$$\begin{aligned} C_{40} &= \mathrm{Cum}(X, X, X, X) = M_{40} - 3M_{20}^2, \\ C_{42} &= \mathrm{Cum}(X, X, X^*, X^*) = M_{42} - \left|M_{20}^2\right| - 2M_{21}^2. \end{aligned} \tag{26}$$

The sixth-order cumulant is

$$\begin{aligned} C_{60} &= \mathrm{Cum}(X, X, X, X, X, X) = M_{60} - 15M_{40}M_{20} + 30(M_{20})^3, \\ C_{63} &= \mathrm{Cum}(X, X, X, X^*, X^*, X^*) = M_{63} - 9M_{42}M_{21} - 6(C_{21})^2. \end{aligned} \tag{27}$$

The eighth-order cumulant is

$$\begin{aligned} C_{80} &= \mathrm{Cum}(X, X, X, X, X, X, X, X), \\ &= M_{80} - 28M_{60}M_{20} - 36M_{40}^2 + 420M_{40}M_{20}^2 - 630M_{40}^4. \end{aligned} \tag{28}$$

Usually, the complex signal of digital social network crisis data disturbed by noise is expressed as follows:

$$s(t) = x(t) + n(t) = \sum_k a_k \sqrt{E} p(t - kT_s) e^{j(2\pi f_c t + \theta_c)} + n(t). \tag{29}$$

Among them, $k = 1, 2, \ldots\ldots, N, N$ represents the length of the transmitted symbol sequence, a_k represents the symbol sequence, $p(t)$ is the baseband waveform, T_s is the symbol duration, E is the signal energy, and the noise $n(t)$ is zero-mean complex white Gaussian noise. The receiver preprocesses the signal to obtain $s(t)$ as follows:

$$s(t) = \sum_k a_k \sqrt{E} p(t - kT_s) e^{j\Delta\theta_c} + n(t). \tag{30}$$

According to the basic principle of the digital social network crisis data signal, a_k in various digital social network crisis data signals can be expressed as follows: the MASK signal is

$$a_k \in \{(2m - 1 - M)d, m = 1, 2, \ldots, M\}, d = \sqrt{\frac{3E}{(M^2 - 1)}}. \tag{31}$$

The MPSK signal is

$$a_k \in \left\{e^{i2\pi(m-1)/M}, m = 1, 2, \ldots, M\right\}. \tag{32}$$

The MFSK signal is

$$a_k = e^{i2\pi f_k t}. \tag{33}$$

Among them, $f_k \in \{(2m - 1 - M)\Delta f/2\pi, m = 1, 2, \ldots, M\}$.

The MQAM signal is

$$a_k = p_k + jq_k = \sqrt{p_k^2 + q_k^2} \times e^{j\phi_k}, \phi_k = \arctan\left(\frac{q_k}{p_k}\right). \tag{34}$$

Among them, $p_k, q_k \in \{(2m - 1 - \sqrt{M})d, m = 1, 2, \ldots, \sqrt{M}\}, d = \sqrt{3/[2(M-1)]}$.

The experiments use the second-, fourth-, sixth-, and eighth-order cumulants of digital social network crisis data signals to generate four high-order cumulant-based features $T1$, $T2$, $T3$, and $T4$, respectively.

$$\begin{aligned} T_1 &= \frac{|C_{40}|}{|C_{21}|^2}, \\ T_2 &= \frac{|C_{40}|}{|C_{42}|} + \frac{|C_{41}|}{|C_{42}|}, \\ T_3 &= \frac{|C_{63}|^2}{|C_{42}|^3}, \\ T_4 &= \frac{|C_{80}|}{|C_{21}|^2}. \end{aligned} \tag{35}$$

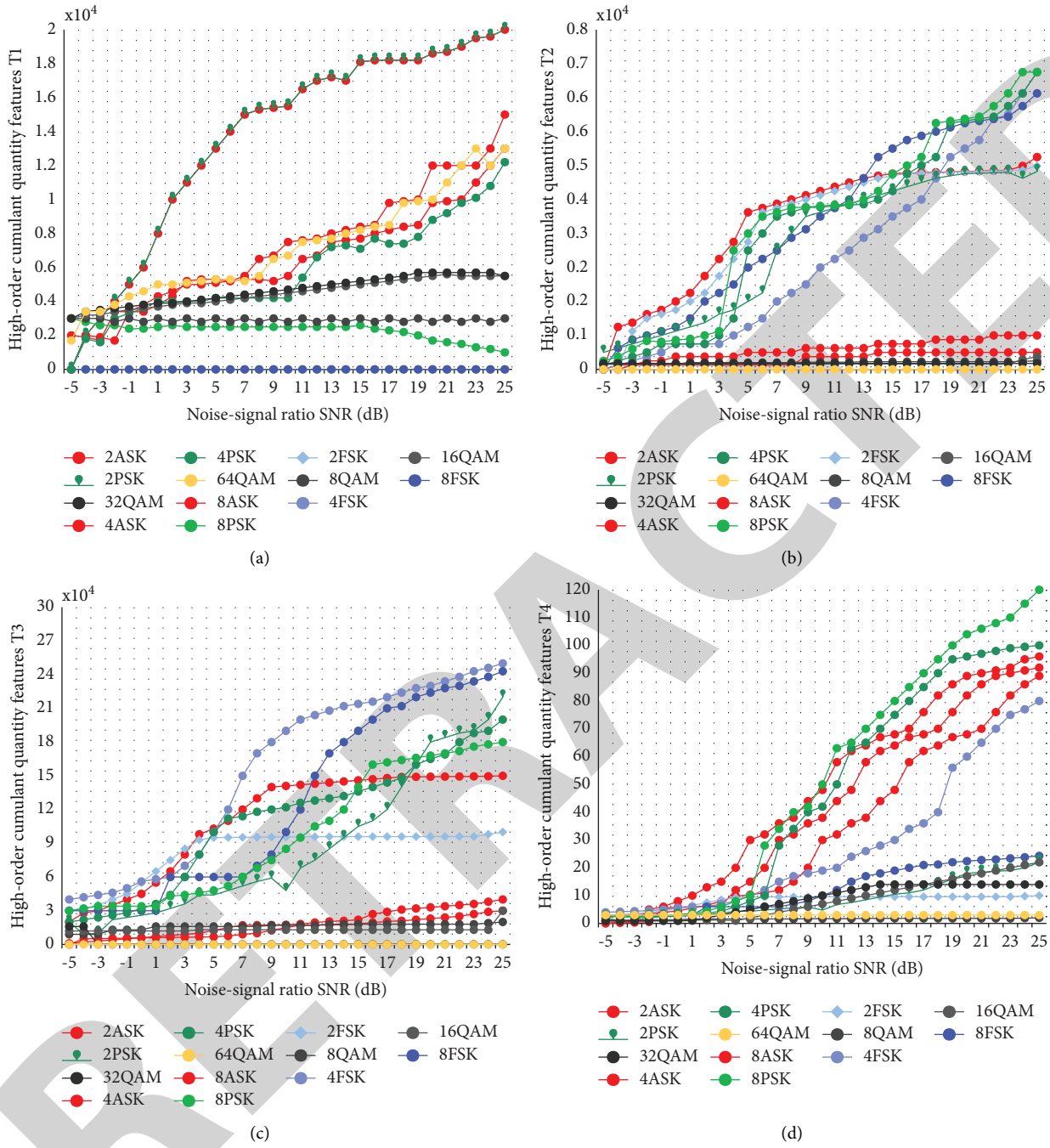

Figure 6: A variation curve of the feature with the signal-to-noise ratio under different social network crisis. (a) A variation curve of the feature T_1 with the signal-to-noise ratio under different social network crisis data methods. (b) A variation curve of the feature T_2 with the signal-to-noise ratio under different social network crisis data methods. (c) A variation curve of the feature T_3 with the signal-to-noise ratio under different social network crisis data methods. (d) A variation curve of the feature T_4 with the signal-to-noise ratio under different social network crisis data methods.

The four high-order cumulant features T_1, T_2, T_3, T_4 of social network crisis data signals vary with the signal-to-noise ratio SNR as shown in Figure 6.

According to theory, the fourth-order cumulant |C40| of the MFSK signal is 0. Based on this characteristic, the MFSK signal can be distinguished from the rest of the social network crisis data signals. The feature T_1 can successfully separate two ASK signals of 4ASK and 8ASK and three kinds of QAM signals of 16QAM, 32QAM, and 64QAM under the condition of SNR > 5 dB. The feature T_2 can completely distinguish the MFSK signal, 2PSK signal, and 4ASK signal when SNR > 15 dB. The feature T_3 has a good identification effect on 2ASK, 2FSK, and 8FSK signals when SNR > −2 dB and can completely distinguish MPSK signals under the

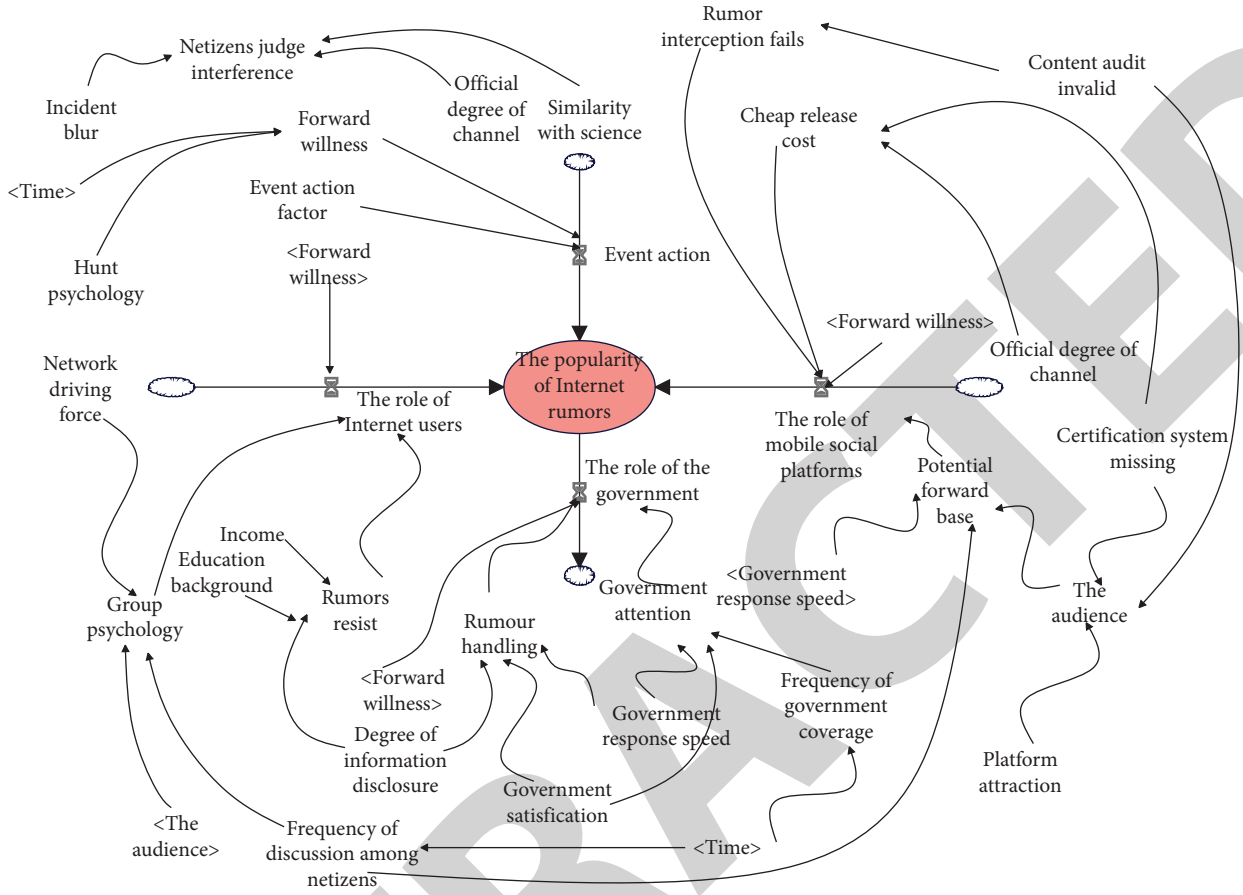

Figure 7: A flow diagram of the rumor-spreading system in the mobile social network.

condition of SNR > 15 dB, and it also has a good distinguishing effect on MFSK and MQAM signals. The feature T_4 has a good effect on distinguishing 13 kinds of social network crisis data signals participating in the experiment. When the SNR > 10 dB, the characteristics of each social network crisis data signal can be clearly separated, and the overall signal differentiation degree is high.

2.3. Transform Domain Feature Parameters. The normalized spectral density is a transform domain feature based on spectral analysis. The spectrum of the signal is P, the normalized spectral density is P_x, and the normalized spectral density statistic S_d obtained by statistical calculation is defined as follows:

$$P_x = \left| \frac{|P|}{E(|P|)} - 1 \right|,$$
$$S_d = \frac{\left| (1/N - 1) \cdot \sum_{n=1}^{N} \left(|P_x(n)| - \overline{P}_x \right)^2 - \overline{P}_x \right|}{\overline{P}_x^2}. \tag{36}$$

The normalized spectral density can effectively realize the distinction between the MASK signal and the MFSK signal. When SNR > 0 dB, the feature S_d can already distinguish MASK signals. In the case of SNR > 15 dB, S_d can accurately separate MASK and MFSK, i.e., two types of social network crisis data signals.

According to the description of the social network crisis data signal, the feature extraction is carried out using the analytical signal sequence $s(i)$ obtained by the social network crisis data signal after the Hilbert transform. The autocorrelation function of $s(i)$ is Fourier transformed, denoted as $A_1(i)$ and then normalized to $A_1(i)$ to obtain the normalized instantaneous amplitude after Fourier transformation, denoted as $A_2(i)$, and the feature A_{auto} is obtained by statistical calculation as follows:

$$A_1(i) = \text{FFT}\{E[s(i)s(i+\tau)]\},$$
$$A_2(i) = \frac{|A_1(i)|}{1/N \sum_{n=1}^{N} |A_1(i)|} - 1, \tag{37}$$
$$A_{\text{auto}} = \frac{D[A_2(i)]}{\{E[A_2(i)]\}^2},$$

When SNR > 3 dB, A_{auto} can distinguish the 2PSK signal and the 8QAM signal, and the discrimination degree of the 2FSK

Table 1: The identification effect and the control effect of the crisis propagation mode based on the social network.

Number	Crisis identification	Crisis control	Number	Crisis identification	Crisis control
1	88.53	79.79	21	86.05	79.18
2	88.69	80.55	22	86.14	77.61
3	86.50	79.09	23	91.88	81.05
4	87.59	77.44	24	87.76	80.81
5	89.73	79.39	25	88.52	80.19
6	87.94	78.75	26	90.77	81.60
7	87.67	81.11	27	91.03	79.05
8	89.46	80.63	28	88.07	81.05
9	88.62	81.69	29	87.44	76.33
10	88.25	76.31	30	87.70	76.98
11	90.37	80.44	31	87.89	79.79
12	91.92	80.28	32	87.27	76.54
13	88.68	76.36	33	88.37	77.61
14	90.98	76.02	34	89.78	80.76
15	90.05	81.82	35	88.35	76.94
16	88.65	77.88	36	87.51	78.36
17	91.65	78.81	37	90.00	76.14
18	86.94	78.94	38	91.12	80.41
19	91.95	76.09	39	89.44	78.10
20	87.30	80.42	40	86.29	77.76

signal is also very high under the high signal-to-noise ratio, and at the same time, it can distinguish large categories of the MASK signal.

P_{auto} is a feature based on the power spectrum of the autocorrelation function. The Fourier transform is performed on the autocorrelation function of $s(i)$ to obtain the power spectrum $C_2(i)$, and then, the standard deviation coefficient is calculated to obtain P_{auto} as follows:

$$\begin{aligned} A_1(i) &= \text{FFT}\{E[s(i)s(i+\tau)]\}, \\ C_2(i) &= \left|A_1(i)\right|^2, \\ P_{\text{auto}} &= \frac{\sigma[C_2(i)]}{E[C_2(i)]} = \frac{\sqrt{D[C_2(i)]}}{E[C_2(i)]}. \end{aligned} \tag{38}$$

The feature P_{auto} has a high degree of discrimination for different signal categories, and the MASK signal and the MFSK signal clearly belong to different regions. The MASK signal can be effectively distinguished when the SNR ≤ 10 dB, and the 8FSK signal can be distinguished from the rest of the MFSK signal when the SNR ≥ 7 dB.

3. Identification Model of the Crisis Propagation Pattern Based on the Social Network

The system flow diagram refers to the model diagram representing the interaction form of each state variable and its flow rate variable and the interconnection between the feedback loops in the whole system. What must be identified in the system flow diagram are the flow level variable and the flow rate variable. The flow level variable refers to a variable with an accumulation effect, its value is the value of the original time plus the variable that occurs when the change occurs, and the flow level variable is changed from the original value to the current time value by the action of the flow rate variable. In addition, flow rate variables are variables that affect state variables that are constantly changing over time. Based on the determined system boundary problem and causal loop diagram analysis, the system flow diagram that affects the spread of online rumors on the mobile social platform is finally determined as shown in Figure 7.

Combined with the algorithm in the second part, the effect of the social network-based crisis propagation model proposed in this paper is verified and the identification effect and control effect of the crisis propagation model are counted, and the results shown in Table 1 are finally obtained.

From the above research, we can see that the crisis propagation model proposed based on the social network in this paper has an obvious effect of identification and control.

4. Conclusion

The research on the dynamics of crisis communication on complex networks has yielded abundant results. However, due to the complexity of network topology and the evolution mechanism of crisis communication in the network crisis communication system, there are still many drawbacks and difficulties in the study of crisis communication dynamics on complex networks. First, most of the current intervention strategies for network crisis communication only consider the topology of the network while ignoring the characteristic information of crisis communication dynamics itself. How to intervene network crisis communication dynamics based on the characteristics of the network structure and the characteristics of crisis communication dynamics itself needs further exploration by scholars. This paper studies the crisis communication mode of social networks, identifies the crisis communication mode through intelligent methods, and builds an intelligent model. Through experimental

research, we can see that the crisis propagation model proposed based on the social network in this paper has an obvious effect of identification and control.

Data Availability

The labeled dataset used to support the findings of this study is available from the corresponding author upon request.

Conflicts of Interest

The author declares no conflicts of interest.

Acknowledgments

This work was supported by Huanghe Jiaotong University.

References

[1] L. Li, Q. Zhang, X. Wang et al., "Characterizing the propagation of situational information in social media during COVID-19 epidemic: a case study on weibo," *IEEE Transactions on computational social systems*, vol. 7, no. 2, pp. 556–562, 2020.

[2] J. I. Criado, A. Guevara-Gómez, and J. Villodre, "Using collaborative technologies and social media to engage citizens and governments during the COVID-19 crisis. The case of Spain," *Digital Government: Research and Practice*, vol. 1, no. 4, pp. 1–7, 2020.

[3] C. Reuter and M. A. Kaufhold, "Fifteen years of social media in emergencies: a retrospective review and future directions for crisis informatics," *Journal of Contingencies and Crisis Management*, vol. 26, no. 1, pp. 41–57, 2018.

[4] M. Mirbabaie, D. Bunker, S. Stieglitz, J. Marx, and C. Ehnis, "Social media in times of crisis: learning from hurricane harvey for the coronavirus disease 2019 pandemic response," *Journal of Information Technology*, vol. 35, no. 3, pp. 195–213, 2020.

[5] D. Zhang, L. Zhou, and J. Lim, "From networking to mitigation: the role of social media and analytics in combating the COVID-19 pandemic," *Information Systems Management*, vol. 37, no. 4, pp. 318–326, 2020.

[6] C. Reuter, A. L. Hughes, and M. A. Kaufhold, "Social media in crisis management: an evaluation and analysis of crisis informatics research," *International Journal of Human-Computer Interaction*, vol. 34, no. 4, pp. 280–294, 2018.

[7] R. Aswani, A. K. Kar, and P. V. Ilavarasan, "Experience: managing misinformation in social media—insights for policymakers from twitter analytics," *Journal of Data and Information Quality (JDIQ)*, vol. 12, no. 1, pp. 1–18, 2020.

[8] M. Eriksson, "Lessons for crisis communication on social media: a systematic review of what research tells the practice," *International Journal of Strategic Communication*, vol. 12, no. 5, pp. 526–551, 2018.

[9] W. Nwankwo and K. E. Ukhurebor, "Web forum and social media: a model for automatic removal of fake media using multilayered neural networks," *International Journal of Scientific and Technology Research*, vol. 9, no. 1, pp. 4371–4377, 2020.

[10] L. Li, Q. Zhang, J. Tian, and H. Wang, "Characterizing information propagation patterns in emergencies: a case study with Yiliang earthquake," *International Journal of Information Management*, vol. 38, no. 1, pp. 34–41, 2018.

[11] T. K. Sell, D. Hosangadi, and M. Trotochaud, "Misinformation and the US Ebola communication crisis: analyzing the veracity and content of social media messages related to a fear-inducing infectious disease outbreak," *BMC Public Health*, vol. 20, no. 1, pp. 550–610, 2020.

[12] J. Yang and S. Lee, "Framing the MERS information crisis: an analysis on online news media's rumour coverage," *Journal of Contingencies and Crisis Management*, vol. 28, no. 4, pp. 386–398, 2020.

[13] X. Wang, Y. Xing, Y. Wei, Q. Zheng, and G. Xing, "Public opinion information dissemination in mobile social networks–taking Sina Weibo as an example," *Information Discovery and Delivery*, vol. 48, no. 4, pp. 213–224, 2020.

[14] S. W. Schuetz, T. A. Sykes, and V. Venkatesh, "Combating COVID-19 fake news on social media through fact checking: antecedents and consequences," *European Journal of Information Systems*, vol. 30, no. 4, pp. 1–13, 2021.

[15] S. Santhoshkumar and L. D. Dhinesh Babu, "Earlier detection of rumors in online social networks using certainty-factor-based convolutional neural networks," *Social Network Analysis and Mining*, vol. 10, no. 1, pp. 20–17, 2020.

[16] M. Mirbabaie, J. Marx, and A. Reimann, "Rumor correction in social media crisis communication: a case of connective sense-breaking," *AIS Transactions on Human-Computer Interaction*, vol. 14, no. 2, pp. 150–184, 2022.

[17] K. Eismann, "Diffusion and persistence of false rumors in social media networks: implications of searchability on rumor self-correction on twitter," *Journal of Business Economics*, vol. 91, no. 9, pp. 1299–1329, 2021.

[18] Y. K. Tse, H. Loh, J. Ding, and M. Zhang, "An investigation of social media data during a product recall scandal," *Enterprise Information Systems*, vol. 12, no. 6, pp. 733–751, 2018.